

Friction Model Based on Tensor Product Transformation

Péter Korondi, Péter Bartal

Department of Automation and Applied Informatics, Budapest Univ. of Technology and Economics, Po. Box: 91, H-1521 Budapest, Hungary, korondi@elektro.get.bme.hu, bartal@elektro.get.bme.hu

Fetah Kolonić

Faculty of Electrical Engineering and Computing, University of Zagreb Unska 3, HR-10000 Zagreb Croatia, fetah.kolonic@fer.hr

Abstract: Friction is a very old and universal issue in all mechanical systems. Since friction is non-linear, it is an ever challenging problem. Several empirical nonlinear friction models have been proposed in the technical literature. This paper does not propose any new model but it presents a new, tensor product (TP) based representation of the existing friction models which is suitable for control design. The TP model transformation is a relatively new method for transforming certain nonlinear models into polytopic model form. The main advantage of the TP model transformation is that the most of the linear state feedback design methods including Linear Matrix Inequality (LMI) can immediately applied to the resulting polytopic models to yield controllers with guaranteed performance.

Keywords: Tensor product, friction compensation

1 Introduction

Friction is omnipresent and a constant issue in any mechanical system. In high precision applications as servo drives for instance, this can be a very annoying issue. Positioning can become really challenging. A proper model for friction could provide relief. However, mechanisms of friction itself are still not fully understood and accurately modelled. Simple linear friction models do not perform well in solving this problem. Nonlinear approaches have also been proposed with more or less success, many of them being based on empirically collected data. It has become obvious that the nonlinear behaviour cannot be modelled using linear models. In this paper a novel approach is presented, based on tensor product (TP)

transformation. The tensor product (TP) model form is a dynamic model representation whereupon Linear Matrix Inequality (LMI) based control design techniques [1]-[3] can immediately be executed. It describes a class of Linear Parameter Varying (LPV) models by the convex combination of linear time invariant (LTI) models, where the convex combination is defined by the weighting functions of each parameter separately. The TP model is not a new model in itself; it is rather a new representation of nonlinear systems that makes the design of the controller much easier. The TP model transformation is a recently proposed numerical method to transform LPV models into TP model form [4]-[6], so that linear control design methods can be applied for the linear components. An important advantage of the TP model forms is that the convex hull of the given dynamic LPV model can be determined and analysed by single variable weighting functions. Furthermore, the feasibility of the LMIs can be considerably relaxed in this representation via modifying the convex hull of the LPV model.

A large number of theoretical models have been elaborated using TP during the last decade; however, few applications have been practically implemented yet, using TP transformations. The aim of the authors is to bridge this gap between theory and application.

The paper has the following structure. The next section briefly presents different friction models, then section 3 introduces the mathematical framework of the TP transformation, section 4 presents the simulations and measured results. Finally section 5 sums up the conclusions.

2 Friction Models Overview

Friction is a physical phenomenon and expressed in quantitative terms as a force F_f , being the force exerted by either of two contacting bodies tending to oppose relative tangential displacement of the other [7]. We can differentiate between three types of friction as *static*, *sliding* and *rolling*. This paper concentrates on the first two forms of occurrence. As apparently no movement occurs we are talking about **static friction**. We talk about **sliding friction**, when the applied force F is great enough to cause sliding. It is found that while the body moves in the direction of F , the friction force is smaller than F , collinear with F and pointing to the opposite direction.

The easiest and probably the most well known model is the so-called **Coulomb friction** model. Though it greatly over simplifies the frictional phenomena it is widely used in the motion control problems, when dynamic effects are not concerned. Also, the Coulomb model is a common piece of all more developed models (see Fig. 1a). The Coulomb friction force F_c is a force of constant magnitude, acting in the direction opposite to motion $v(t)$.

$$\text{When } v(t) \neq 0: F_f(t) = -F_c \text{sign}(v(t)) \quad (1)$$

$$F_c = \mu F_N, \quad (2)$$

where F_N is the normal component of the force pressing surfaces together and μ is the frictional factor. μ is determined by measurements under certain conditions. One of the biggest problems of the Coulomb model is, that it cannot handle the vicinity of zero velocity, hence the properties of motion at starting or zero velocity crossing, i.e. static and rising static friction F_s . To apply the model for those cases a $\mu_0 > \mu$ factor has been introduced.

$$\text{When } v(t) = 0: F_f(t) \leq F_s = \mu_0 F_N \quad (3)$$

At motion start, it replaces μ in (2) until the process arrives to steady state. The values of μ and μ_0 can be found in any major physics or engineering tabulations for different material pairs in both dry and lubricated conditions. The first tabulations of those kinds date back to the beginning of 18th century.

The **viscous friction** element models the friction force as a force proportional to the sliding velocity:

$$\text{When } v(t) \neq 0: F_f(t) = -F_v v(t) \quad (4)$$

where F_v is the coefficient of viscous friction.

The model is used for the friction caused by the viscosity of the fluids, specifically lubricants. A combination with Coulomb friction yields (see Fig. 1b):

$$\text{When } v(t) \neq 0: F_f(t) = -F_v \cdot |v|^{\delta_v} \text{sign}(v(t)), \quad (5)$$

where δ_v is a geometry-dependent parameter. The model can be refined by adding the influence of an external force for the friction at rest. This, however, leads to a discontinuous function (see Fig. 1c). Here, an important contribution has been made by Stribeck. Armstrong-Hélouvy proposed a model which involves a nonlinear [8], but continuous function (see Fig. 1d):

$$\text{When } v(t) \neq 0: F_f(t) = - \left(F_C + (F_s - F_C) \cdot e^{-\frac{|v|}{v_s} \delta} \right) \text{sign}(v(t)) - F_v \cdot v \quad (6)$$

where v_s is the Stribeck velocity, δ is an empirical parameter, F_s is the static friction force. A similar model was employed by Hess and Soom [9].

$$\text{When } v(t) \neq 0: F_f(t) = - \left(F_C + \frac{(F_s - F_C)}{1 + (v/v_s)^2} \right) \text{sign}(v(t)) - F_v v \quad (7)$$

The Stribeck curve is an advanced model of friction as a function of velocity (see

Fig. 1d). Although it is still valid only in steady state, it includes the model of Coulomb, static and viscous friction as built-in elements. There are several more advanced models in the technical literature. This paper does not intend to introduce any new friction model. Only a new representation of the existing models is proposed which is suitable for controller design.

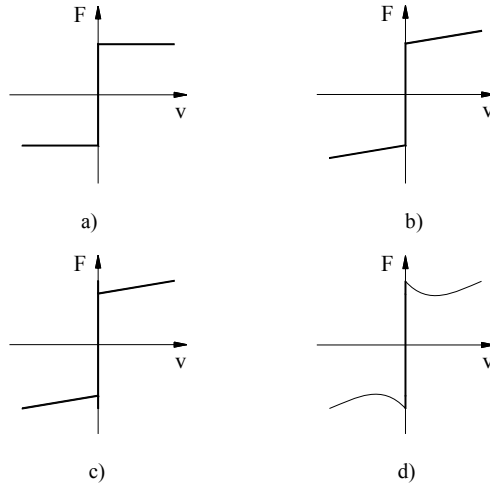


Figure 1

Different friction curves (friction vs. velocity): a) Coulomb friction, b) Coulomb and viscous friction, c) influence of an external force in case of friction at rest added to the viscous friction, d) Stribeck curve

3 Theoretical Background of the TP Transformation

Consider a parametrically varying dynamical system:

$$\begin{aligned}\dot{\mathbf{x}}(t) &= \mathbf{A}(\mathbf{p}(t))\mathbf{x}(t) + \mathbf{B}(\mathbf{p}(t))\mathbf{u}(t) \\ \mathbf{y}(t) &= \mathbf{C}(\mathbf{p}(t))\mathbf{x}(t) + \mathbf{D}(\mathbf{p}(t))\mathbf{u}(t)\end{aligned}\quad (8)$$

with input $\mathbf{u}(t) \in \mathfrak{R}^m$, output $\mathbf{y}(t) \in \mathfrak{R}^l$ and state vector $\mathbf{x}(t) \in \mathfrak{R}^k$. The system matrix is a parameter-varying object, where $\mathbf{p}(t) \in \Omega$ is a time varying N -dimensional parameter vector, and is an element of the closed hypercube $\Omega = [a_1, b_1] \times [a_2, b_2] \times \dots \times [a_N, b_N] \in \mathfrak{R}^N$. The parameter $\mathbf{p}(t)$ can also include some elements of $\mathbf{x}(t)$. Given the LPV system description in (8), it can be reformulated using:

$$\mathbf{S}(\mathbf{p}(t)) = \begin{pmatrix} \mathbf{A}(\mathbf{p}(t)) & \mathbf{B}(\mathbf{p}(t)) \\ \mathbf{C}(\mathbf{p}(t)) & \mathbf{D}(\mathbf{p}(t)) \end{pmatrix} \in \mathfrak{R}^{(k+m) \times (k+l)} \quad (9)$$

thus:

$$\begin{pmatrix} \dot{\mathbf{x}}(t) \\ \mathbf{y}(t) \end{pmatrix} = \mathbf{S}(\mathbf{p}(t)) \begin{pmatrix} \mathbf{x}(t) \\ \mathbf{u}(t) \end{pmatrix} \quad (10)$$

The final goal of TP model transformation is to express (10) in tensor product form considering different optimization and convexity constraints.

3.1 Basic Steps of TP Model Transformation

The details are in [4]-[6], here only the main idea is summarized briefly, since an open matlab toolbox is available at [10] for performing the numerical calculation. The basic idea is illustrated in Fig. 2 for case of $N=1$.

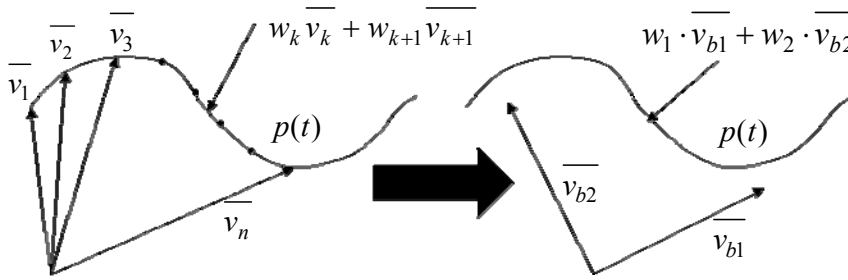


Figure 2
Basic idea TP model transformation

The $p(t)$ is sampled in n points by vectors \bar{v}_k . Between the sampled points, $p(t)$ is approximated by interpolation. It is well known that $p(t)$ can be described by two orthogonal base vectors \bar{v}_{b1} and \bar{v}_{b2} in a properly selected coordinate system. This simple idea is generalized for TP transformation.

In the first step, the transformation generates a discrete finite element TP model form from the system which can be described by analytical formulas, soft-computing models, or real-world measurement data. For analytical and soft-computing models it is performed by numerical discretization over a hyper-rectangular grid, whilst for measurement data the measurement process is designed to directly result the discrete finite element TP model. The system is known in the discrete points and an interpolation technique is necessary between the discrete points. The explicit form of the tensor product then becomes

$$\begin{pmatrix} \dot{\mathbf{x}}(t) \\ \mathbf{y}(t) \end{pmatrix} \approx \left(\sum_{i_1=1}^{I_1} \sum_{i_2=2}^{I_2} \dots \sum_{i_N=1}^{I_N} \prod_{n=1}^N w_{n,i_n} (p_n(t)) \mathbf{S}_{i_1,i_2,\dots,i_N} \right) \begin{pmatrix} \mathbf{x}(t) \\ \mathbf{u}(t) \end{pmatrix} \quad (11)$$

where there are $R = \prod_{n=1}^N I_n$ vertex discrete LTI systems denoted $\mathbf{S}_{i_1, i_2, \dots, i_N} \in \mathfrak{R}^{(k+m) \times (k+l)}$ and the row vector $w_{n, i_n}(p_n(t)) \in \mathfrak{R}^{I_n}$ is the i_n^{th} weighting or interpolation function belonging to the n^{th} dimension of $\mathbf{\Omega}$ and $p_n(t)$ is the n^{th} element of the $\mathbf{p}(t)$ vector. I_n denotes the number of weighting functions used in the n^{th} dimension of $\mathbf{\Omega}$. Note that the dimensions of $\mathbf{\Omega}$ are respectively assigned to the elements of the parameter vector $\mathbf{p}(t)$.

The Tensor Product (TP) model transformation is a uniform, numerical method. It is capable of transforming uniformly both in a theoretical way and as an applied algorithm the linear parameter-varying dynamic models (8) into parameter-varying weighted combination of parameter independent (constant) system models (linear time-invariant systems) (11) taking into account different optimization and convexity constraints. Usually, there is no prior information on how the optimal LTI vertex systems can be selected, that is why density of the grids of the discrete system is usually high at the first step. The next step is the extraction of the minimal number of LTI vertex systems by HOSVD-reduction [11].

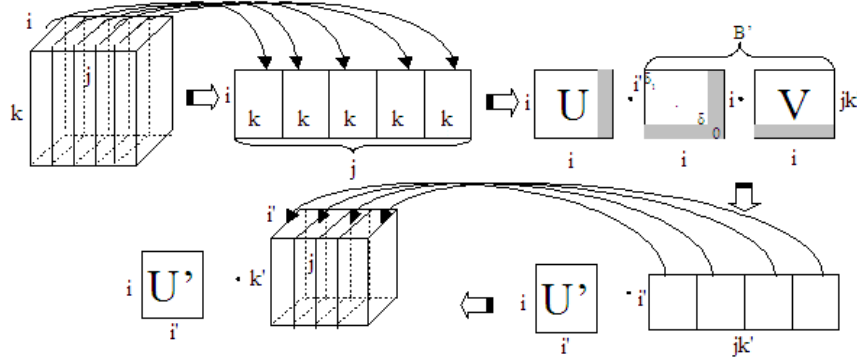


Figure 3
HOSVD decomposition

It is known from matrix algebra, that each matrix can be written in the form:

$$\mathbf{A} = \mathbf{U} \cdot \mathbf{\Lambda} \cdot \mathbf{V} \quad (12)$$

where \mathbf{A} is an arbitrary $n \times m$ matrix, \mathbf{U} is a matrix that contains the eigenvectors of the matrix $\mathbf{A} \cdot \mathbf{A}^T$; $\mathbf{\Lambda}$ contains the so called singular values in its diagonal. \mathbf{V} contains the eigenvectors of the matrix $\mathbf{A}^T \cdot \mathbf{A}$ again. $\mathbf{\Lambda}$ is a diagonal matrix, often denoted as a vector. The occurrence of zeros in matrix $\mathbf{\Lambda}$ allows us to decrease the size of matrix \mathbf{A} . In case of a tensor, it has to be unfolded into bidimensional space, to form an ordinary matrix (first step in Fig. 3), then the singular value decomposition (SVD) can be applied, thus obtaining a simplified system. Finally the matrix must be packed back into its original tensor form. The above operations

can be performed along every dimension (Fig. 3), ensuring the best possible reduction of the system, resulting finally in a higher order singular value decomposition (HOSVD).

4 Application

The experimental system consists of a conventional DC servo gear motor with encoder feedback and variable inertia load coupled by a relatively rigid shaft, as shown in Fig. 4. The controller is implemented using a DSP as the computation engine detail description is in [12].

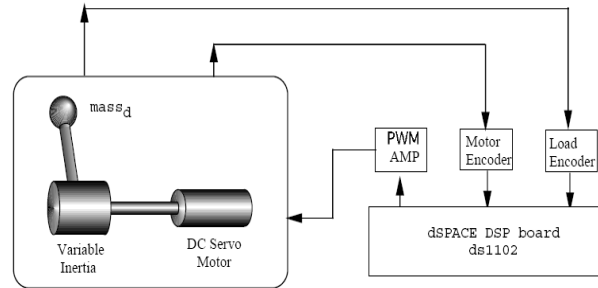


Figure 4
The experimental system

During the control design, the flexibility of the shaft was ignored as well as friction. The state variables are the shaft position, θ , the shaft angular velocity, ω , and the armature current, i , the control signal is the motor voltage u .

$$\begin{pmatrix} \dot{\theta} \\ \dot{\omega} \\ \dot{i} \end{pmatrix} = \begin{pmatrix} 0 & 1 & 0 \\ 0 & 0 & \frac{K_t}{J} \\ 0 & -\frac{K_\omega}{L_a} & -\frac{R_a}{L_a} \end{pmatrix} \begin{pmatrix} \theta \\ \omega \\ i \end{pmatrix} + \begin{pmatrix} 0 \\ 0 \\ \frac{1}{L_a} \end{pmatrix} u \quad (13)$$

Here J is the inertia of the motion control system, K_t and K_ω are the torque constant and the back-EMF constant, respectively, R_a and L_a are the resistance and the inductance of the armature. The effect of $mass_d$ is considered as a disturbance. The viscous, Coulomb and Stribeck frictions were modelled by (7) in the following way,

$$\dot{\omega} = - \underbrace{\frac{F_v}{J}\omega}_{\text{viscous term}} - \underbrace{\left(\frac{2F_c}{J(1+e^{-500\omega})} - \frac{F_c}{J}\right)}_{\text{Coulomb term}} - \underbrace{\left(\frac{2(F_s - F_c)}{1+e^{-500\omega}} - (F_s - F_c)\right)}_{\text{Stribeck term}} + \underbrace{\frac{K_t}{J}i}_{\text{term for electric torque}} \quad (14)$$

where the second two terms are nonlinear and the signum function is approximated as

$$\text{sign}(\omega) = \frac{2}{(1+e^{-500\omega})} - 1 \quad (15)$$

F_v was given in the data sheet of the servo motor, F_c , F_s and ω_s were determined through testing. Fig. 5 shows the simulated Stribeck curve. The model calculated from the rated parameters of the system is:

$$\begin{pmatrix} \dot{\theta} \\ \dot{\omega} \\ \dot{i} \end{pmatrix} = \begin{pmatrix} 0 & 1 & 0 \\ 0 & p(t) & 42 \\ 0 & -4600 & -2450 \end{pmatrix} \begin{pmatrix} \theta \\ \omega \\ i \end{pmatrix} + \begin{pmatrix} 0 \\ 0 \\ 1100 \end{pmatrix} u \quad (16)$$

$$p(t) \equiv p(\omega) = -\frac{F_v}{J} - \frac{2F_c}{\omega J(1+e^{-500\omega})} - \frac{F_c}{\omega J} - \frac{2(F_s - F_c)}{1+e^{-500\omega}} - \frac{(F_s - F_c)}{\omega J(1+(\omega/\omega_s)^2)} \quad (17)$$

where $\Omega = [\omega_{\min}, \omega_{\max}] = [-4, 4]$ Since equidistant sampling is applied and the sampling density must be high around zero velocity, the interval Ω is sampled at 1370 grid points (even number is necessary to avoid division by zero). The sampled system is arranged into a tensor

$$\mathbf{S}_\omega = (\mathbf{A}_1 \quad \mathbf{B}_1 \quad \cdots \quad \mathbf{A}_{1370} \quad \mathbf{B}_{1370}) \in \mathfrak{N}^{1370 \times 4 \times 2}, \quad (18)$$

where tensor \mathbf{S}_ω , has only two singular values ($197.32 \cdot 10^3$ and $10.61 \cdot 10^3$). That is why the above nonlinear system can be modelled by two linear systems (it is a significant reduction of $\mathbf{S}_\omega \in \mathfrak{N}^{1370 \times 4 \times 2}$):

$$\mathbf{A}^1 = \begin{pmatrix} 0 & 1 & 0 \\ 0 & -20.2 & 42 \\ 0 & -4600 & -2450 \end{pmatrix}; \quad \mathbf{A}^2 = \begin{pmatrix} 0 & 1 & 0 \\ 0 & -6239 & 42 \\ 0 & -4600 & -2450 \end{pmatrix}; \quad \mathbf{B}^1 = \mathbf{B}^2 = \begin{pmatrix} 0 \\ 0 \\ 1100 \end{pmatrix} \quad (19)$$

The weightings ($w_1(\omega)$ and $w_2(\omega)$) are functions of the velocity as shown in Fig. 6. The shape of the weighting functions is quite straightforward to explain. The nonlinear friction terms are modelled using a varying viscosity coefficient, which is represented by the a_{22} element in the system matrix. \mathbf{A}^1 with small viscous

coefficient dominates at high speed, where the Coulomb friction is relatively small. The \mathbf{A}^2 system matrix with very large viscous coefficient dominates at low speed, where the Coulomb friction is comparatively large.

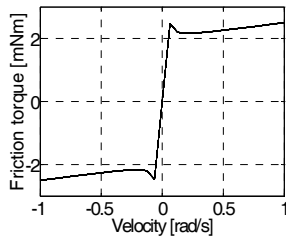


Figure 5
 Simulated Stribeck curve

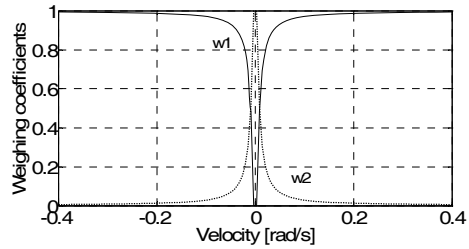


Figure 6
 The weighting coefficients as function of velocity

To verify the TP based model, the real and simulated velocities (ω_r , ω_s) are compared in Fig. 7, where the input voltage of the motor is a shifted sinusoid with an amplitude of 12 V (open loop response). The value of the input voltage is divided by 5 to plot the velocity and input voltage in the same figure. One kind of nonlinearity of the system stems from the huge friction of the harmonic gear. It can be seen in Fig. 7 that if the motor is at standstill, at least 2 V need to be switched across the motor to start it. On the other hand, the motor sticks, if the input voltage is under 1.2 V. According to Fig. 7, the simulated model is acceptable from an engineering point of view.

The power electronic PWM unit is saturated at 22 V. It is also a kind of nonlinearity which could be handled using a TP model. Because this paper concentrates on friction, only the nonlinearity of the friction is considered.

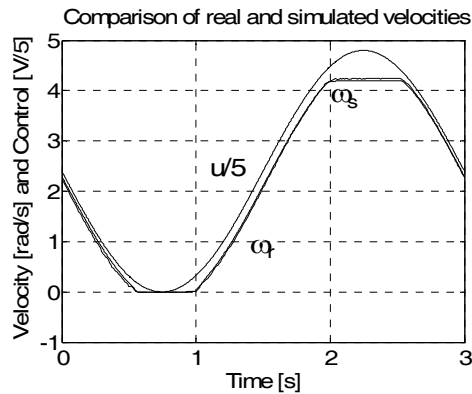


Figure 7
 Open loop responses for sinusoidal input voltage

Three cases have been examined by simulation. In all cases, the system has the following initial state:

$$\theta = -0.1 \text{ rad}, \quad \omega = 0 \text{ rad/sec and } i = 0 \text{ A.}$$

The aim of the controller is to move all state variables to 0.

Case 1 (Linear Model-Linear Feedback: LM-LF)

The servo system is modelled by a simple linear time invariant system $(\mathbf{A}^1 \ \mathbf{B}^1)$, which models only the linear (viscous) friction. The state feedback controller is designed by pole placement. The poles of the closed loop system are selected as

$$\text{Pole} = [-1 \ -1750 \ -2500] \quad (20)$$

The feedback gains are arranged in a row vector

$$u = -\mathbf{K}_{lin} \mathbf{x}, \text{ where } \mathbf{K}_{lin} = [94.6970 \ 88.7573 \ 1.6189] \quad (21)$$

Case 2 (Nonlinear Model-Linear Feedback: NM-LF)

The model of servo system is extended by nonlinear Coulomb and Stribeck terms, according to (16) and (17) but the controller is the same as in the previous case.

Case 3 (Nonlinear Model-Tensor Product Feedback: NM-TP)

The servo system is modelled by (16) and (17) as in the previous case. A TP based feedback controller is design for the TP model (19). Two feedback vectors \mathbf{K}_1 and \mathbf{K}_2 are calculated by pole placement for both systems $(\mathbf{A}^1 \ \mathbf{B}^1)$ and $(\mathbf{A}^2 \ \mathbf{B}^2)$ in a way that the poles of both closed loop systems are the same as (20). The control is calculated as the convex combination of the state-feedbacks of the two component systems in the following way:

$$u = -\left(\sum_{r=1}^2 w_r(\omega) \mathbf{K}_r \right) \mathbf{x} \quad (22)$$

$$\text{where } \mathbf{K}_1 = \mathbf{K}_{lin} \text{ and } \mathbf{K}_2 = [94.6970 \ 359.0732 \ -4.0345]$$

The performances of these three cases are compared in Fig. 8. The Case 1, LM-LF is considered as the reference, i.e. the performance of a pure linear system with the closed loop poles of (20). It is clear that if the same linear state-feedback is applied and the model is extended by nonlinear terms, the system response is slower in Case 2, NM-LF. Because of the nonlinear terms, the servomotor will get stuck before it reaches its desired position and a constant steady state error remains. In case of a linear system, the steady state error can be eliminated by an integral term but the Coulomb friction might cause the well known stick slip phenomenon. The main advantage of the TP based control (NM-TP) is that it can eliminate the steady sate error without stick slip phenomenon, see Case 3, NM-TP in Fig 8.

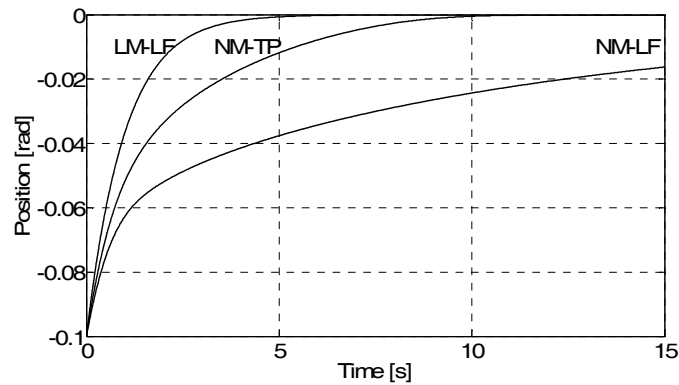


Figure 8
Closed loop responses of three systems

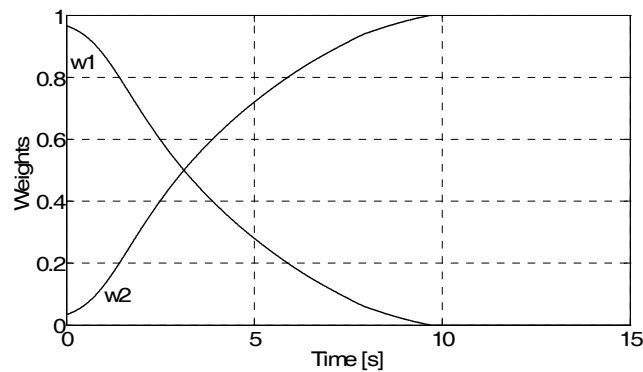


Figure 9
Time functions of the weightings

Conclusion

This paper proposed a new approach for modelling the friction. It proved that this new approach is promising in the sense of the application of a linear control design method for a system which has nonlinearity because of the friction. The open Matlab toolbox performs the steps of Tensor Product based model transformation automatically.

Acknowledgement

The authors wish to thank the National Science Research Fund (OTKA K62836), Control Research Group and János Bolyai Research Scholarship of Hungarian Academy of Science for their financial support and the support stemming from the Intergovernmental S & T Cooperation Program.

References

- [1] S. Boyd, L. E. Ghaoui, E. Feron, V. Balakrishnan: Linear matrix inequalities in system and control theory, *Philadelphia PA:SIAM, ISBN 0-89871-334-X*, 1994
- [2] P. Gahinet, A. Nemirovski, A. J. Laub, M. Chilali: *LMI Control Toolbox*. The MathWorks, Inc., 1995
- [3] C. W. Scherer, S. Weiland: *Linear Matrix Inequalities in Control*, ser. DISC course lecture notes, DOWNLOAD:
<http://www.cs.ele.tue.nl/SWeiland/lmid.pdf>, 2000
- [4] P. Baranyi: TP model transformation as a way to LMI based controller design, *IEEE Transaction on Industrial Electronics*, Vol. 51, No. 2, pp. 387-400, April 2004
- [5] Zoltán Petres, Barna Reskó, Péter Baranyi: TP Model Transformation Based Control of the TORA System, *Production Systems and Information Engineering*, 2:159-175, 2004
- [6] P. Baranyi, P. Korondi, R. J. Patton, H. Hashimoto: Trade-off Between Approximation Accuracy and Complexity for TS fuzzy Models, *Asian Journal of Control*, Vol. 6. No. 1, Issue 21, March, 2004, pp. 21-33
- [7] Rabinowicz, E., 1965, *Friction and Wear of Materials*, John Wiley and Sons, NY
- [8] Armstrong-Hélouvry, B., Dupont, P., de Wit, C. C. (1994b): A Survey of Models, Analysis Tools and Compensation Methods for the Control of Machines with Friction, *Automation* **30**(7), 1083-1138
- [9] Hess, D. P., Soom, A. (1990): Friction at a Lubricated Line Contact Operating at Oscillating Sliding Velocities, *J. of Tribology* 112(1), 147-152
- [10] <http://www.sztaki.hu/tpdc> or
https://wiki.sztaki.hu/cogvis/index.php/Tensor_Product_Model_Transformation_based_Controller_Design_Framework
- [11] Lieven De Lathauwer, Bart De Moor, Joos Vandewalle: A Multilinear Singular Value Decomposition, *SIAM Journal on Matrix Analysis and Applications*, 21(4):1253-1278, 2000
- [12] P. Korondi, H. Hashimoto: Sliding Mode Design for Motion Control, *Studies in Applied Electromagnetics and Mechanics* Vol. 16, ISBN 90 5199 487 7, IOS Press, 2000